Research Article

Quality and Reliability Engineering International

(wileyonlinelibrary.com) DOI: 10.1002/qre.1286

Published online 10 January 2012 in Wiley Online Library

On the Monitoring of Simple Linear Berkson Profiles

Yi-Hua Tina Wang and Longcheen Huwang*,†

We consider the quality of a process, which can be characterized by a simple linear Berkson profile. One existing approach for monitoring the simple linear profile and two new proposed schemes are studied for charting the simple linear Berkson profile. Simulation studies demonstrate the effectiveness and efficiency of one of the proposed monitoring schemes. In addition, a systematic diagnostic approach is provided to spot the change point location of the process and to identify the parameter of change in the profile. Finally, an example from semiconductor manufacturing is used to illustrate the implementation of the proposed monitoring scheme and diagnostic approach. Copyright © 2012 John Wiley & Sons, Ltd.

Keywords: average run length; change point; control chart; EWMA; generalized likelihood ratio

1. Introduction

Statistical process control (SPC) has been successfully applied in a variety of industries. In most SPC applications, the quality of a process can be adequately represented by the distribution of a quality characteristic. However, in many applications, the quality of a process or product may be better characterized by a relationship (or profile) between the response variable and one or more explanatory variables; that is, the main topic is on monitoring the profile that describes such a relationship, instead of on monitoring a single quality characteristic. Particularly, most studies focused on the simple linear profiles. An extensive discussion of research problems on this topic has been provided by Woodall *et al.*[1]

Kang and Albin[2] proposed two kinds of control charting schemes for monitoring the simple linear profiles in Phase I and Phase II. One is a multivariate T^2 chart and the other is the combination of a exponentially weighted moving average (EWMA) chart and a range (R) chart. Kim *et al.*[3] proposed using a combination of three EWMA charts to, respectively, detect a shift in the intercept, slope, and standard deviation simultaneously in Phase II. They also suggested using similar Shewhart-type control charts for monitoring simple linear profiles in Phase I. Gupta *et al.*[4] compared the performance of the control charts proposed by Croarkin and Varner[5] and Kim *et al.*[3] for monitoring simple linear profiles in Phase II. They concluded that the combined EWMA charts of Kim *et al.*[3] are superior to Croarkin and Varner's[5] charting scheme. Mahmoud and Woodall[6] studied several control charting schemes for monitoring simple linear profiles in Phase I. Zou *et al.*[7] proposed a control charting scheme based on a change point model for monitoring simple linear profiles where the process parameters are unknown but can be estimated from the in-control historical data. On the basis of likelihood ratio statistics, Mahmoud *et al.*[8] proposed a change point method for monitoring sustained shifts in a simple linear profile in Phase I. Zou *et al.*[9] used a self-starting control chart for monitoring simple linear profiles when the process parameters are unknown but some in-control data in Phase I are available. For monitoring general linear profiles, Zou *et al.*[10] applied an MEWMA single chart to the transformations of estimated profile parameters in Phase II. More studies related to monitoring linear profiles can be found in the literature (see e.g. Jensen *et al.*,[11] Mestek *et al.*,[12] Stover and Brill,[13] and Lawless *et al.*[14]).

In many practical situations, the profile cannot be represented adequately by a linear model. Walker and Wright[15] and Woodall *et al.*[1] studied the vertical density profile, which apparently cannot be represented by a linear profile. Williams *et al.*[16] developed three general approaches to the formulation of T^2 statistics based on nonlinear model approach in Phase I. Colosimo and Pacella[17] used principal component analysis to identify systematic patterns in roundness profiles. Williams *et al.*[18] used data from DuPont to monitor dose–response profiles used in high-throughput screening based on the nonlinear model approach of Williams *et al.*[16], in which a four-parameter logistic regression model was used to represent the profiles. Jin and Shi[19] used dimension-reduction techniques to study a stamping tonnage profile, which apparently is a nonlinear profile. Lada *et al.*[20] and Ding *et al.*[21] used dimension–reduction techniques, including wavelet and independent component analysis to study a general category of nonlinear profiles.

Institute of Statistics, National Tsing Hua University, Hsinchu, 30043, Taiwan.
**Correspondence to: Longcheen Huwang, Institute of Statistics, National Tsing Hua University, Hsinchu, 30043, Taiwan.*
†E-mail: huwang@stat.nthu.edu.tw

Recently, Zou *et al.*[22] integrated an MEWMA procedure with a generalized likelihood ratio test (Fan *et al.*[23]) based on local linear regression of Fan and Gijbels[24] to monitor a general smooth regression profile. Qiu *et al.*[25] proposed monitoring smooth profiles, which can be described by a nonparametric mixed-effects model to account for the within-profile correlation.

In this article, we focus on a study of Phase II method for monitoring a simple linear regression-like profile which can be well represented by a simple linear Berkson Model. To be specific, assume that for the jth random sample collected overtime, we have the observations (x_{ij}, y_{ij}), where y_{ij} is the response variable and x_{ij} is the controllable variable. For each controllable variable x_{ij}, there exists a latent variable ξ_{ij}, which equals x_{ij} minus a random error δ_{ij}, that has a linear relationship with the response variable y_{ij}. Precisely, the underlying model is as follows:

$$\begin{aligned} y_{ij} &= A_0 + A_1\xi_{ij} + \varepsilon_{ij}, \\ x_{ij} &= \xi_{ij} + \delta_{ij}, i = 1, 2, \cdots, n, j = 1, 2, \cdots, \end{aligned} \tag{1}$$

where ξ_{ij} is the unobserved latent variable. The controllable variable x_{ij} is usually the assigned value of an experiment and hence is the same for different j. In the article, we will use x_i to replace x_{ij} for brevity. The variable δ_{ij} represents the random error between the controllable variable x_i and the latent variable ξ_{ij}, which is independent of x_i and ε_{ij}. Furthermore, it is assumed that $\varepsilon_{ij} \sim^{i.i.d.} N\left(0, \sigma_\varepsilon^2\right)$ and $\delta_{ij} \sim^{i.i.d.} N\left(0, \sigma_\delta^2\right)$. Equation (1) is called the simple linear Berkson model, which was first proposed by Berkson.[26] Without further assumptions, it is obvious that the parameters A_0, A_1, σ_ε^2, and σ_δ^2 in Equation (1) cannot be estimated consistently. To identify Equation (1), it is usually assumed that the variance of δ_{ij}, σ_δ^2, is known a priori, or it can be independently estimated by certain extra data. Throughout this article, we assume that σ_δ^2 is a known constant, not a parameter.

A model, which can also be formulated by Equation (1), is called the simple linear measurement error model. However, the simple linear Berkson model and the simple linear measurement error model are remarkably different. In the former model, the random error δ_{ij} is independent of the controllable variable x_i, whereas in the later model the random error δ_{ij} is correlated with the observable variable x_{ij} (note that x_{ij} is different for different j in the simple linear measurement error model). The simple linear Berkson model is useful and can be applied in many different applications including engineering, agriculture, medical study, and so forth. For example, assume that we are conducting an experiment on the quality of cement being created in a continuous mixing operating. Assume that the quality of cement is a linear function of the amount of water used in the mixture. We can set the reading on the dial of a water valve controlling water entering the mixture. However, because of random fluctuations in water pressure, the amount of water actually delivered per unit of time is not that set on the dial, and it is not accessible either. Thus, the true amount of water is equal to the amount set on the water dial minus a random error. If the dial has been calibrated properly, the average of the random error is zero. It is also commonly assumed that the random error has a normal distribution. As a result, the above problem should be better described by the simple linear Berkson Equation (1), instead of the simple linear model. Another example of the simple linear Berkson Equation (1) is yield of corn and total amount of nitrogen absorption. It can be shown roughly that the yield of corn has a linear relationship with the total amount of nitrogen that the corn absorbs from soil. However, the true unobserved amount of nitrogen that has been absorbed by the corn is quite different from the quantity of nitrogen that has been applied on per unit of land. Thus, it is better to use the simple linear Berkson model to present the problem, instead of using the simple linear regression model. Berkson model has been widely used in many different applications (see e.g. Rosner *et al.*,[27] Rosner *et al.*,[28] Tosteson *et al.*,[29] and Schafer and Gilbert[30]).

In the article, the main purpose is to monitor the simple linear Berkson profile (Equation (1)). The rest of the article is organized as follows. In Section 2, we review one existing method proposed by Zou *et al.*[22] for monitoring the simple linear profiles that can be used to monitor the simple linear Berkson profiles. We also present two new charting schemes for monitoring the simple linear Berkson profiles. Then, we compare the monitoring performance of the two proposed charts with that of Zou *et al.*[22] in Section 3. In Section 4, we provide a systematic method for profile diagnosis and evaluate the performance of the proposed estimate of change point and the tests for identifying the parameter of change. In Section 5, we use an industrial example from semiconductor manufacturing, which has a profile that fits a simple linear Berkson model well, to demonstrate, the step-by-step implementation of the proposed approach. Conclusions and summaries are included in Section 6. Theoretical derivations are given in Appendix A.

2. Phase II monitoring

Substituting $x_i - \delta_{ij}$ for ξ_{ij} in Equation (1) and using the coded controllable values, we obtain the following alternative form of Equation (1):

$$y_{ij} = B_0 + B_1 x_i^* + \varepsilon_{ij}^*, i = 1, 2, \cdots, n, j = 1, 2, \cdots, \tag{2}$$

where $B_0 = A_0 + A_1\bar{x}, B_1 = A_1, x_i^* = x_i - \bar{x}, \bar{x} = \sum_{i=1}^n x_i/n, \varepsilon_{ij}^* = \varepsilon_{ij} - B_1\delta_{ij} \sim^{i.i.d.} N(0, \sigma^2)$, and $\sigma^2 = \sigma_\varepsilon^2 + B_1^2\sigma_\delta^2$. Note that under the assumptions of the simple linear Berkson Equation (1), the error term ε_{ij}^* does not depend on the controllable values x_i^*. As a result, Equation (2) itself can be treated as a simple linear model. However, the variance of the error term ε_{ij}^* in Equation (2) has been augmented from σ_ε^2, the variance of the error term ε_{ij} in Equation (1), to $\sigma^2 = \sigma_\varepsilon^2 + B_1^2\sigma_\delta^2$. It is worth noting that although the simple linear Berkson Equation (1) can be treated as the simple linear Equation (2), the parameters which we are interested in detecting possible changes are A_0, A_1, and σ_ε^2, not B_0, B_1, and σ^2. On the basis of some preliminary study, it does not seem very effective to directly monitor the parameters A_0, A_1, and σ_ε^2 in Equation (1). The reason is that the consistent estimators of A_1 and σ_ε^2 are not mutually independent. As a result, for monitoring σ_ε^2, the control limits based on the consistent estimator of σ_ε^2 depend on the values of A_1 and σ_δ^2, and hence the resulting charting scheme is not regression invariant. As an alternative, to monitor simple linear Berkson profile (1) that has three

parameters A_0, A_1, and σ_ε^2 to be controlled can be accomplished through monitoring the parameters B_0, B_1, and σ^2 in the simple linear profile (2). This is the approach we will take in the rest of the article.

For the jth profile in the Phase II monitoring, $j = 1, 2, \cdots$, the least squares estimators for B_0, B_1, and σ^2 in Equation (2) are

$$\hat{B}_{0j} = \bar{y}_j, \hat{B}_{1j} = \frac{S_{xy(j)}}{S_{xx}}, \text{and } \hat{\sigma}_j^2 = \frac{1}{n-2}\sum_{i=1}^{n}\left(y_{ij} - \hat{B}_{0j} - \hat{B}_{1j}x_i^*\right)^2, \tag{3}$$

where $\bar{y}_j = \sum_{i=1}^{n} y_{ij}/n$, $S_{xx} = \sum_{i=1}^{n}(x_i - \bar{x})^2$, and $S_{xy(j)} = \sum_{i=1}^{n}(x_i - \bar{x})y_{ij}$. Note that the above three least squares estimators $\hat{B}_{0j}$, $\hat{B}_{1j}$, and $\hat{\sigma}_j^2$ are mutually independent, and it is also well known that control charting schemes based on these estimators are regression invariant. In the following, we will present one existing chart and propose two new charting schemes on monitoring B_0, B_1, and σ^2 in Equation (2).

2.1. ZTW control chart

Zou *et al.*[22] applied an MEWMA scheme to the transformations of estimated profile parameters to form a single chart for monitoring both the coefficients and the variance of a general linear profile. In the simple linear Equation (2), let $\mathbf{Z}_j = \left(Z_{1j}, Z_{2j}, Z_{3j}\right)'$, where $Z_{1j} = \left(\hat{B}_{0j} - B_0\right)/\sigma$, $Z_{2j} = \left(\hat{B}_{1j} - B_1\right)/\sigma$, and $Z_{3j} = \Phi^{-1}\left\{F\left[(n-2)\hat{\sigma}_j^2/\sigma^2, n-2\right]\right\}$. Here, $\Phi^{-1}(\cdot)$ is the inverse of the standard normal distribution function and $F(\cdot, \nu)$ is the distribution function of a chi-square random variable with ν degrees of freedom. One advantage of the scheme of Zou *et al.*[22] is that only one single chart is used to monitor all of the profile parameters so that the design and implementation of the monitoring scheme can be greatly simplified. Also, the variance transformation Z_{3j} has nice properties that its distribution is independent of the sample size n when the process is in control, and thus the choice of its control limits will not be affected by n. This will help design the control chart easily in the case of variable sample size. Note that this kind of variance transformation has been used in EWMA control charts proposed by Quesenberry[31] and Chen *et al.*[32] When the process is in control, $\mathbf{Z}_j$ is a three-dimensional multivariate normal distribution with mean $\mathbf{0}$ and covariance matrix Σ=diag$(1/n, 1/S_{xx}, 1)$. Zou *et al.*[22] used the EWMA charting statistic

$$\mathbf{W}_j = \lambda\mathbf{Z}_j + (1-\lambda)\mathbf{W}_{j-1},$$

where $\mathbf{W}_0 = 0$ and λ, $(0 < \lambda \leqslant 1)$, is a smoothing constant. The control chart (designated as the ZTW control chart) signals if

$$U_j = \mathbf{W}_j'\Sigma^{-1}\mathbf{W}_j > L_{ZTW}\frac{\lambda}{(2-\lambda)} \tag{4}$$

where $L_{ZTW} > 0$ is determined to achieve a desired in-control (IC) ARL. The ZTW control chart is a special application of MEWMA charts, which were first proposed by Lowry *et al.*[33]

2.2. HWYC control charts

Huwang *et al.*[34] proposed an EWMA chart as a way on monitoring variance of a univariate quality characteristic for individual observations. Here, we generalize the idea to propose an EWMA chart for monitoring the variance of the simple linear Equation (2) with sample size $n > 1$. For monitoring the intercept and slope of the simple linear Equation (2), we adopt the two EWMA charts of Kim *et al.*[3] for these two parameters. Denote

$$\text{EWMA}_I(j) = \lambda\hat{B}_{0j} + (1-\lambda)\text{EWMA}_I(j-1)$$

and

$$\text{EWMA}_S(j) = \lambda\hat{B}_{1j} + (1-\lambda)\text{EWMA}_S(j-1),$$

where $\text{EWMA}_I(0) = B_0$ and $\text{EWMA}_S(0) = B_1$. Consequently, the lower and upper control limits for the monitoring statistics $\hat{B}_{0j}$ and $\hat{B}_{1j}$ are

$$\text{LCL}_I, \text{UCL}_I = B_0 \pm L_I\sigma\sqrt{\frac{\lambda}{(2-\lambda)n}} \tag{5}$$

and

$$\text{LCL}_S, \text{UCL}_S = B_1 \pm L_S\sigma\sqrt{\frac{\lambda}{(2-\lambda)S_{xx}}}$$

respectively, where L_I and L_S are chosen to achieve a specified IC ARL. The three EWMA charts (denoted as the HWYC charts in the article) will be used jointly, and the profile change is detected as one of the charts signals.

Using the approach similar to Huwang *et al.*[34], for the *j*th sample, we first define the EWMA statistic

$$\begin{aligned}\mathrm{EWMA}_\chi(j) &= \lambda\frac{(n-2)\hat{\sigma}_j^2}{\sigma^2} + (1-\lambda)\mathrm{EWMA}_\chi(j-1)\\ &= \sum_{i=1}^{j}\lambda(1-\lambda)^{j-i}\frac{(n-2)\hat{\sigma}_i^2}{\sigma^2} + (1-\lambda)^j\mathrm{EWMA}_\chi(0)\end{aligned}$$

where $(n-2)\hat{\sigma}_i 2/\sigma^2$ has a chi-square distribution with $n-2$ degrees of freedom when the process is in control and $\mathrm{EWMA}_\chi(0) = n-2$. Using the result of Box[35] (Theorem 3.1), the term $\left[\mathrm{EWMA}_\chi(j) - (1-\lambda)^j(n-2)\right]\lambda^{-1} = \sum_{i=1}^{j}(1-\lambda)^{j-i}(n-2)\hat{\sigma}_i^2/\sigma^2$ can be approximated by a gamma distribution with shape parameter $q_j/2$ and scale parameter $2p_j$, where

$$p_j = \frac{\sum_{i=0}^{j-1}(1-\lambda)^{2i}}{\sum_{i=0}^{j-1}(1-\lambda)^{i}} = \frac{1+(1-\lambda)^j}{(2-\lambda)}$$

$$q_j = \frac{\left[\sum_{i=0}^{j-1}(n-2)(1-\lambda)^i\right]^2}{\sum_{i=0}^{j-1}(n-2)(1-\lambda)^{2i}} = \frac{(n-2)(2-\lambda)\left[1-(1-\lambda)^j\right]}{\lambda\left[1+(1-\lambda)^j\right]}$$

Further, it is well known (Lawless[36]) that the log transformation of a gamma distribution is approximately normally distributed. Thus,

$$T_j = ln\left[\frac{\mathrm{EWMA}_\chi(j) - (1-\lambda)^j(n-2)}{\lambda}\right] \approx N\left[\mathrm{E}(T_j), \mathrm{Var}(T_j)\right],$$

where

$$\mathrm{E}(T_j) \approx ln(p_j q_j) - \frac{1}{q_j} - \frac{1}{3q_j^2} + \frac{2}{15q_j^4},$$

$$\mathrm{Var}(T_j) \approx \frac{2}{q_j} + \frac{2}{q_j^2} + \frac{4}{3q_j^3} - \frac{16}{15q_j^5}.$$

Consequently, the lower and upper control limits for the monitoring statistic T_j are

$$\begin{aligned}\mathrm{LCL}_{\mathrm{HWYC}} &= \mathrm{E}(T_j) - L_{1,\mathrm{HWYC}}\sqrt{\mathrm{Var}(T_j)},\\ \mathrm{UCL}_{\mathrm{HWYC}} &= \mathrm{E}(T_j) + L_{2,\mathrm{HWYC}}\sqrt{\mathrm{Var}(T_j)},\end{aligned} \tag{6}$$

where $L_{1,\mathrm{HWYC}}$ and $L_{2,\mathrm{HWYC}} > 0$ are chosen to achieve a specified IC ARL. The major difference between this approach and most of others (e.g. Shu and Jiang[37]) for monitoring σ^2 is that up to the *j*th sample, the HWYC approach only uses two approximations to establish the EWMA charting scheme, whereas usually *j* approximations are used for the other EWMA charts to develop the charting scheme. The parsimonious use of approximation in deriving the monitoring statistic T_j is likely to lead to a more efficient control chart. Huwang *et al.*[34] used this approach to propose an EWMA chart to detect variance change of a univariate quality characteristic for individual observations. Their ARL comparisons show that for monitoring increase in variance their EWMA chart is as good as the change point CUSUM chart of Acosta-Mejia.[38] On the other hand, for monitoring decrease in variance, their EWMA chart is uniformly better than the change point CUSUM chart.

2.3. *COM control charts*

On the basis of some preliminary simulation studies, it is known that the transformation $Z_{3j} = \Phi^{-1}\left\{F\left[(n-2)\hat{\sigma}_j^2/\sigma^2, n-2\right]\right\}$ used in the ZTW chart is very efficient in detecting increase in variance σ^2 (see also Quesenberry[31] and Chen *et al.*[32]). On the other hand, the control chart for monitoring σ^2 defined in the HWYC charts is significantly better than other charts in detecting decrease in variance σ^2 (Huwang *et al.*[34]). Thus, it is intuitive to combine these two one-sided charts as a two-sided chart for monitoring σ^2.

Define

$$\mathrm{EWMA}_{C^+}(j) = \lambda Z_{3j} + (1-\lambda)\mathrm{EWMA}_{C^+}(j-1),$$

where $\mathrm{EWMA}_{C^+}(0) = 0$. Then this chart will detect an increase in σ^2 if

$$\mathrm{EWMA}_{C^+}(j) > \mathrm{UCL}_{\mathrm{COM}} = L_{2,\mathrm{COM}}\sqrt{\frac{\lambda}{2-\lambda}},$$

where $L_{2,\mathrm{COM}}$ is chosen to achieve a specified IC ARL. As for monitoring decrease in σ^2, the monitoring statistic $\mathrm{EWMA}_{C^-}(j) = T_j$ defined in the HWYC charts is adopted with the corresponding lower control limit

$$\mathrm{LCL}_{\mathrm{COM}} = \mathrm{E}(T_j) - L_{1,\mathrm{COM}}\sqrt{\mathrm{Var}(T_j)}, \tag{7}$$

where $L_{1,\mathrm{COM}}$ is determined to achieve a desired IC ARL. Here, we combine two one-sided charts as a two-sided chart for monitoring changes in σ^2. The combined EWMA chart for monitoring σ^2 will be jointly used with the two EWMA charts of Kim *et al.*[3] (defined in Section 2.2) for monitoring the intercept and slope to detect profile changes. The resulting charts will be called the COM control charts throughout, and a profile change is triggered if any one of the charts signals.

3. Performance comparisons

In this section, we compare the performance of the three competing control charts for monitoring the simple linear Berkson profile (Equation (1)) in terms of ARL. For simplicity, we only consider the zero-state out-of-control (OC) ARL. Assume that when the variance of δ_i, σ_δ^2, equals 0, the in-control simple linear Berkson profile is the same as the in-control simple linear model of Kang and Albin,[2] where the parameters are $A_0 = 3$, $A_1 = 2$, $\sigma_\varepsilon^2 = 1$ and $x_i = 2, 4, 6, 8$. Here, the known variance σ_δ^2 is considered to be 0.1 and 0.25, and the smoothing constant for all EWMA charts is chosen to be 0.2 as consistent with the commonly used value in the literature. The overall IC ARL is roughly equal to 200 with equally distributed to all three EWMA charts for the intercept, slope, and variance. For example, each separate EWMA chart of the COM scheme for monitoring the intercept B_0, or the slope B_1, or the variance σ^2 in Equation (2) has the same individual IC ARL and the two one-sided EWMA charts for monitoring increase and decrease in σ^2, respectively, also have the same individual IC ARL.

Table I presents the L values for the three competing control charts when the overall IC ARL is approximately equal to 200 based on 20,000 Monte Carlo simulations. Note that the L values for all control charts do not vary with σ_δ^2 because of regression invariance property.

The OC ARLs of the three competing charts for detecting shifts in A_0, A_1, and σ_ε are given in Table II for $\sigma_\delta^2 = 0.1$, which represents a little difference between the controllable variable x and the latent variable ξ. When A_0 is changed to $A_0 + c_I\sigma_\varepsilon$, except for $c_I = 0.1$ or -0.1, the COM charts perform best among the three charts, but overall all charts have quite similar results. For detecting shifts in A_1, the ZTW chart is uniformly better than the other two charts although the results of all three charts are not significantly different for larger shifts. Note that unlike in the simple linear profile where the ARL performance of a commonly used chart for detecting increase or decrease in slope is approximately the same, it is not the case in the simple linear Berkson model because of the relationship $\sigma^2 = \sigma_\varepsilon^2 + A_1^2\sigma_\delta^2$. With increase shifts in σ_ε, the ZTW chart gives better results than the other two charts in all cases considered especially for smaller increases. As for detecting decrease shifts in σ_ε, all control charts are biased procedures. A control chart is called a biased procedure if it has the property that some OC ARL is greater than the IC ARL. Despite the undesirable bias of the HWYC charts when the decrease shift is small, they are uniformly better than the ZTW chart, and the advantage is dramatic when the decrease shift is large. On the other hand, the COM charts give the second best results and as expected the results are not remarkably different from those of the HWYC charts. Note that it is possible to rectify bias of the HWYC charts (COM charts as well) by using two unequal-tailed one-sided charts jointly to monitor the parameter σ_ε. However, it could be numerically cumbersome to search for two unequal-tailed one-sided charts to make the combined chart unbiased (see e.g. Acosta-Mejia and Pignatiello Jr.[39]). As a result, unbiased charting schemes are not pursued in the article. On the contrary, because the ZTW scheme uses a single chart to monitor all parameters together, it is impossible to modify the ZTW chart to make it unbiased.

Table III presents the OC ARLs of the three competing charts for detecting shifts in A_0, A_1, and σ_ε^2 for $\sigma_\delta^2 = 0.25$, which represents a slightly larger difference between the controllable variable x and the latent variable ξ. The results show that except for few cases in detecting decrease shifts in σ_ε^2, all charts have larger OC ARLs for detecting the same shifts in A_0, A_1, and σ_ε^2 as compared with their counterparts in Table II, respectively. For detecting shifts in A_0, the COM charts still give the best results in most cases, but the differences among the three charts are not significant. As for detecting shifts in A_1, the ZTW chart performs slightly better than the other two charts, but the results for all three charts do not have much difference when the shifts get larger. For detecting increase shifts in σ_ε, the ZTW chart gives better results than the other two charts especially for smaller increases. As for detecting decrease shifts in σ_ε, the HWYC charts are uniformly better than the other two charts, although all charts give OC ARLs greater than the IC ARL in some cases. The results of the HWYC and COM charts are not remarkably different. On the contrary, both the HWYC and COM charts significantly outperform the ZTW chart especially for larger decreases.

Table I. The L values for the three control charts when $\mathrm{ARL}_0 \approx 200$

	ZTW		HWYC	COM
ARL_0	200.02		199.52	200.11
	(0.88)		(1.41)	(1.42)
L_{ZTW}	11.855	L_I	3.016	3.016
		L_S	3.011	3.011
		L_σ^+	2.792	3.055
		L_σ^-	3.031	3.038

Parentheses contain the standard errors.

Table II. OC ARL*s* of the three competing charts for $A_0 \rightarrow A_0 + c_I\sigma_\varepsilon$, $A_1 \rightarrow A_1 + c_S\sigma_\varepsilon$, and $\sigma_\varepsilon \rightarrow c_\varepsilon\sigma_\varepsilon$ when σ_δ^2=0.1 in Equation (1)

					c_I					
	0.10	0.20	0.30	0.40	0.50	0.60	0.80	1.00	1.50	2.00
ZTW	145.07	75.48	39.70	23.48	15.50	11.18	7.02	5.11	3.11	2.31
HWYC	146.61	74.69	37.93	21.96	14.36	10.28	6.45	4.66	2.85	2.14
COM	146.93	74.60	37.91	21.91	14.34	10.28	6.45	4.66	2.85	2.14
	−0.10	−0.20	−0.30	−0.40	−0.50	−0.60	−0.80	−1.00	−1.50	−2.00
ZTW	146.83	76.89	40.07	23.51	15.43	11.24	7.06	5.14	3.13	2.32
HWYC	148.03	75.99	38.35	22.18	14.35	10.33	6.46	4.71	2.87	2.15
COM	148.42	75.96	38.34	22.16	14.33	10.32	6.46	4.71	2.87	2.15
					c_S					
	0.025	0.0375	0.05	0.0625	0.075	0.10	0.125	0.15	0.20	0.25
ZTW	112.84	70.91	45.06	30.73	21.89	12.97	8.85	6.71	4.50	3.44
HWYC	115.80	72.84	46.54	31.30	22.44	13.27	9.07	6.81	4.56	3.47
COM	115.66	72.62	46.46	31.28	22.42	13.25	9.05	6.81	4.56	3.47
	−0.025	−0.0375	−0.05	−0.0625	−0.075	−0.10	−0.125	−0.15	−0.20	−0.25
ZTW	120.00	75.99	48.62	32.66	22.88	13.35	9.10	6.82	4.57	3.47
HWYC	122.45	77.78	49.51	33.10	23.45	13.57	9.22	6.90	4.60	3.48
COM	122.77	77.82	49.47	33.09	23.42	13.56	9.22	6.90	4.60	3.48
					c_ε					
	1.10	1.15	1.20	1.25	1.30	1.40	1.60	1.80	2.20	2.60
ZTW	99.78	69.58	49.58	36.75	28.14	18.37	10.02	6.78	4.10	2.96
HWYC	108.32	78.26	57.67	43.34	33.53	21.88	11.94	7.95	4.69	3.36
COM	106.16	75.84	55.00	40.96	31.39	20.40	11.12	7.43	4.46	3.22
	0.95	0.90	0.85	0.80	0.75	0.70	0.65	0.60	0.55	0.50
ZTW	256.35	290.20	287.30	253.23	209.25	167.15	131.46	102.86	80.52	63.76
HWYC	238.79	238.03	194.97	140.10	94.99	65.10	45.49	33.17	25.14	19.70
COM	241.52	241.40	198.16	142.02	96.22	65.86	46.05	33.49	25.32	19.87

Table III. OC ARL*s* of the three competing charts for $A_0 \rightarrow A_0 + c_I\sigma_\varepsilon$, $A_1 \rightarrow A_1 + c_S\sigma_\varepsilon$, and $\sigma_\varepsilon \rightarrow c_\varepsilon\sigma_\varepsilon$ when σ_δ^2=0.25 in Equation (1)

					c_I					
	0.10	0.20	0.30	0.40	0.50	0.60	0.80	1.00	1.50	2.00
ZTW	157.97	94.55	53.52	32.67	21.57	15.37	9.27	6.57	3.82	2.76
HWYC	159.65	94.58	52.11	31.01	20.19	14.24	8.54	6.03	3.50	2.54
COM	160.17	94.56	52.06	30.96	20.16	14.22	8.54	6.03	3.50	2.54
	−0.10	−0.20	−0.30	−0.40	−0.50	−0.60	−0.80	−1.00	−1.50	−2.00
ZTW	159.40	95.87	54.65	32.90	21.61	15.34	9.35	6.59	3.84	2.78
HWYC	160.70	95.57	53.03	31.31	20.21	14.23	8.58	6.05	3.52	2.55
COM	161.59	95.67	52.98	31.28	20.17	14.21	8.58	6.05	3.52	2.55
					c_S					
	0.025	0.0375	0.05	0.0625	0.075	0.10	0.125	0.15	0.20	0.25
ZTW	126.76	86.83	58.03	40.69	29.67	17.42	11.78	8.67	5.66	4.23
HWYC	130.33	89.32	60.28	41.93	30.38	17.96	12.10	8.92	5.79	4.30
COM	130.42	88.94	60.01	41.80	30.32	17.93	12.08	8.90	5.79	4.30
	−0.025	−0.0375	−0.05	−0.0625	−0.075	−0.10	−0.125	−0.15	−0.20	−0.25
ZTW	140.55	97.59	66.65	46.13	33.18	18.96	12.50	9.11	5.85	4.33
HWYC	141.78	99.17	68.14	47.01	33.67	19.32	12.66	9.23	5.89	4.34
COM	142.23	99.27	68.09	46.97	33.63	19.30	12.64	9.23	5.89	4.34
					c_ε					
	1.10	1.15	1.20	1.25	1.30	1.40	1.60	1.80	2.20	2.60
ZTW	122.74	94.59	72.78	56.30	44.36	29.19	15.60	9.97	5.64	3.93
HWYC	130.84	103.81	81.36	64.96	51.99	34.61	18.51	11.87	6.59	4.49
COM	129.15	101.47	78.88	62.26	49.36	32.50	17.24	11.04	6.16	4.28
	0.95	0.90	0.85	0.80	0.75	0.70	0.65	0.60	0.55	0.50
ZTW	239.16	273.33	291.29	291.98	279.26	254.99	229.51	202.65	179.66	158.30
HWYC	229.72	244.24	236.37	210.93	176.69	141.98	113.28	89.98	72.86	60.00
COM	231.81	247.12	240.19	214.32	179.27	144.36	114.73	91.27	73.84	60.67

From the results of Tables II and III, we conclude that overall, the COM charts have the best performance for detecting shifts in A_0; the ZTW chart gives the best results for detecting shifts in A_1; the ZTW chart performs better than the other two charts for detecting increase shifts in σ_ε, but it has the worst performance for detecting decrease shifts in σ_ε; and the HWYC charts outperform the other two charts for detecting decrease shifts in σ_ε, although they give poor results for detecting increase shifts in σ_ε. For detecting decrease shifts in σ_ε, the results of the COM and HWYC charts are not remarkably different and the COM charts outperform the HWYC charts in almost all other situations; consequently, in the following, only the COM charts and the ZTW chart will be compared as we consider simultaneous shifts in two parameters.

To make performance comparisons in detecting simultaneous shifts in the intercept and slope consistent with those in the literature, here we consider the simultaneous shifts in the two parameters of B_0, B_1, and σ_ε instead of A_0, A_1, and σ_ε. Note that Kim *et al.*[3] and Zou *et al.*[10] considered the same parameters B_0 and B_1 of the transformed simple linear model on monitoring simple linear profiles. Table IV tabulates the OC ARLs of the ZTW chart and the COM charts for several simultaneous shifts in B_0 and B_1, B_0 and σ_ε, and B_1 and σ_ε when $\sigma_\delta^2 = 0.1$. With increase shifts in both B_0 and B_1, in some situations the ZTW chart is superior to the COM charts, whereas in other situations the ZTW chart is inferior to the COM charts. Overall, their results are not appreciably different. As with increase shifts in both B_0 and σ_ε, except for the cases where $c_I \leqslant 0.15$ and $c_\varepsilon \leqslant 1.3$ that the ZTW chart is noticeably better than the COM charts, the results of both charts are not quite different in the other situations. For detecting the combination of an increase shift in B_1 and a decrease shift in σ_ε, the COM charts are uniformly better than the ZTW chart. In some situations, the advantage of the COM charts over the ZTW chart is dramatic. For example, when $c_S = 0.025$ and $c_\varepsilon = 0.8$, the OC ARL of the COM charts is 143.62, which is much smaller than 235.31 of the ZTW chart. As for detecting the combination of a decrease shift in B_1 and an increase shift in σ_ε, except for few cases ($c_S \geqslant -0.075$ and $c_\varepsilon \leqslant 1.3$) that the advantage of the ZTW chart over the COM charts is appreciable, in other situations the results of both charts are not different much. For each of the other combinations of simultaneous shifts in two parameters, the results (not reported here) are similar to those of one combination of simultaneous shifts in two parameters in Table IV. In conclusion, if the simultaneous shifts do not contain a decrease in σ_ε, in a few cases the ZTW chart is slightly better than the COM charts whereas in most cases the results of both charts are not appreciably different. On the other hand, if the simultaneous shifts contain a decrease in σ_ε, the COM charts are uniformly better than the ZTW chart and the superiority is dramatic in some cases. Furthermore, we also simulated the OC ARLs of the ZTW and COM charts for several simultaneous shifts in two parameters for the situation that $\sigma_\delta^2 = 0.25$. Under the same simultaneous shifts scenarios, both charts have larger OC ARLs as compared with the results in the situation that $\sigma_\delta^2 = 0.1$. However, the conclusions are quite similar to those of $\sigma_\delta^2 = 0.1$. Hence the results are not reported.

From the results in Tables 2–4, overall if both single shifts in one parameter and simultaneous shifts in two parameters are considered, the COM charts are slightly preferable to the ZTW chart.

4. The diagnostic aids and implementation

In the practical quality applications, it is not only important to detect process change as soon as possible but also critical to diagnose the change and identify which parameter or parameters in the model have shifted after an OC signal appeared. To search for the change point and to identify the type of parameter change in the model, a diagnostic aid will help an engineer isolate and eliminate the assignable causes of a problem fast and easily. In the following we, study the diagnosis of a simple linear Berkson model and propose a systematic diagnostic method to find the location of the change point and which parameters in the model that have shifted.

To find an estimate of the change point in a simple linear Berkson model, a maximum likelihood estimation approach is used. Once an OC signal is found at sample k by a control chart, the estimate of the change point τ of a sustained shift is given by

$$\widetilde{\tau} = \underset{0 \leqslant t < k}{\textbf{argmax}} \{lr(tn, kn)\} \tag{8}$$

where $lr(tn, kn)$ is the generalized likelihood ratio statistic. The definition of the term $lr(tn, kn)$ and the derivation of the estimate $\widetilde{\tau}$ are included in Appendix A. The generalized likelihood ratio test approach has been used for change point detection in general linear models and nonparametric regression models in the literature of SPC (see e.g. Hawkins *et al.*,[40] Hawkins and Zamba,[41,42] Zou *et al.*,[7] Zou *et al.*,[9] Mahmoud *et al.*,[8] Zou *et al.*,[22] and Zou *et al.*[10]). Pignatiello and Samuel[43] showed that the maximum likelihood method performs much better than other methods for change point detection for a conventional process change. Note that to calculate the estimate $\widetilde{\tau}$ in Equation (8), we have to find the maximum likelihood estimates of B_0, B_1, and σ_ε^2 for $0 \leqslant t < k$, respectively. Because of the relationship $\sigma^2 = \sigma_\varepsilon^2 + B_1^2\sigma_\delta^2$, the maximum likelihood estimate of σ_ε^2 is not equal to $\hat{\sigma}^2 - \hat{B}_1^2\sigma_\delta^2$ when the condition $\hat{\sigma}^2 - \hat{B}_1^2\sigma_\delta^2 < 0$ holds, where $\hat{B}_1$ and $\hat{\sigma}^2$ are the maximum likelihood estimates of B_1 and σ^2, respectively. As a result, it is more complex and statistical skill oriented to derive the result of Equation (8).

In the literature of Economics, there have been several studies on change point detection of a linear model using maximization of the generalized likelihood ratio. The change points include changes of coefficient parameters and/or standard deviation in the model (see e.g. Andrew,[44] Bai,[45] Csörgő and Horváth,[46] Liu *et al.*,[47] Bai,[48] Bai and Perron[49,50]). Under more general assumptions than previous studies, Qu and Perron[51] used the approach of maximizing the generalized likelihood ratio to obtain the estimator(s) of change point (s) in the general linear model. The limiting distribution of the estimator of the change point is obtained as well. Here, we use the approach of Qu and Perron[51] to show that

Table IV. OC ARLs of the ZTW chart (first row) and the COM charts (second row) under any two combinations of $B_0 \to B_0 + c_l\sigma_\varepsilon$, $B_1 \to B_1 + c_S\sigma_\varepsilon$, and $\sigma_\varepsilon \to c_\varepsilon\sigma_\varepsilon$ for σ_δ^2=0.1 in Equation (2)

					c_S					
	0.025	0.05	0.075	0.10	0.125	0.15	0.175	0.20	0.225	0.25	
	0.05	160.55	119.55	84.10	58.13	40.80	29.99	22.69	17.85	14.51	12.18
		162.15	122.38	85.36	58.02	40.26	28.98	21.88	16.98	13.73	11.42
	0.10	129.26	100.91	74.46	52.82	38.15	28.50	21.61	17.41	14.18	11.87
		132.88	104.97	76.58	54.11	38.40	28.13	21.47	16.75	13.58	11.33
	0.15	97.55	79.88	61.18	45.88	34.47	26.14	20.46	16.58	13.58	11.47
		99.47	82.90	64.21	47.92	35.40	26.67	20.73	16.37	13.37	11.20
	0.20	70.98	59.90	48.50	38.16	29.64	23.26	18.76	15.25	12.82	10.93
		70.55	62.14	51.65	40.72	31.77	24.76	19.65	15.79	13.04	10.99
	0.25	51.85	45.60	37.87	31.06	25.36	20.49	17.12	14.30	12.16	10.49
c_l		50.57	46.46	40.38	34.00	27.74	22.49	18.29	15.02	12.58	10.70
	0.30	37.88	34.82	30.27	25.82	21.58	18.25	15.36	13.08	11.28	9.90
		36.97	34.86	31.78	27.97	23.86	20.03	16.76	14.17	11.99	10.34
	0.35	29.33	27.07	24.40	21.25	18.44	15.83	13.73	11.99	10.54	9.28
		27.97	26.83	25.16	22.86	20.26	17.60	15.22	13.15	11.35	9.93
	0.40	23.00	21.78	19.80	17.72	15.74	13.83	12.25	10.85	9.66	8.72
		21.69	21.10	20.14	18.73	17.16	15.46	13.74	12.12	10.65	9.46
	0.45	18.34	17.54	16.42	15.07	13.74	12.33	11.05	9.91	9.02	8.15
		17.34	17.00	16.48	15.69	14.64	13.52	12.28	11.08	9.95	8.96
	0.50	15.19	14.70	13.89	12.97	11.93	11.02	9.88	9.11	8.32	7.63
		14.26	14.07	13.77	13.25	12.63	11.85	10.98	10.09	9.23	8.40
						c_ε					
	1.10	1.20	1.30	1.40	1.50	1.60	1.80	2.20	2.60	3.00	
	0.05	93.34	48.19	27.83	18.06	13.10	10.11	6.77	4.10	2.97	2.34
		100.42	52.81	30.81	20.18	14.43	11.04	7.41	4.46	3.22	2.54
	0.10	80.68	43.52	26.35	17.81	12.74	9.91	6.67	4.06	2.97	2.34
		85.25	48.22	29.15	19.47	14.12	10.87	7.34	4.44	3.21	2.54
	0.15	64.38	38.37	23.96	16.47	12.26	9.64	6.61	4.02	2.95	2.34
		67.94	41.66	26.83	18.46	13.63	10.60	7.25	4.42	3.20	2.54
	0.20	50.28	32.83	21.89	15.55	11.78	9.39	6.43	4.06	2.93	2.33
		52.28	35.24	24.05	17.25	13.03	10.29	7.14	4.38	3.19	2.53
	0.25	39.10	26.76	19.26	14.37	11.10	8.96	6.40	4.01	2.93	2.32
c_l		39.94	29.41	21.29	15.91	12.35	9.93	6.98	4.35	3.18	2.53
	0.30	30.57	22.85	16.98	13.05	10.49	8.51	6.16	3.92	2.90	2.31
		30.85	24.31	18.64	14.55	11.57	9.49	6.82	4.31	3.16	2.52
	0.35	23.95	19.03	14.90	11.87	9.70	8.13	5.99	3.89	2.88	2.31
		24.43	20.22	16.33	13.19	10.77	9.02	6.64	4.25	3.14	2.51
	0.40	19.97	16.30	13.30	10.97	9.10	7.74	5.87	3.84	2.85	2.31
		19.60	16.96	14.29	11.95	10.04	8.56	6.45	4.20	3.13	2.50
	0.45	16.30	13.92	11.79	10.02	8.53	7.24	5.61	3.80	2.86	2.29
		16.14	14.42	12.61	10.85	9.32	8.07	6.23	4.14	3.11	2.49
	0.50	13.93	12.09	10.57	9.10	7.92	6.89	5.46	3.71	2.83	2.27
		13.50	12.43	11.11	9.83	8.62	7.62	6.00	4.07	3.08	2.48
						c_ε					
		0.95	0.90	0.85	0.80	0.75	0.70	0.65	0.60	0.55	0.50
	0.025	221.91	255.42	258.80	235.31	198.67	161.48	127.44	101.74	80.24	64.28
		214.00	222.91	191.67	143.62	99.52	68.92	48.34	35.33	26.55	20.76
	0.05	160.24	186.58	195.83	184.79	162.35	137.02	111.34	92.40	73.75	60.34
		157.14	170.95	160.38	132.14	98.24	70.14	50.09	36.89	27.70	21.66
	0.075	107.14	121.87	131.45	132.35	122.72	107.58	91.42	77.92	64.32	52.70
		104.55	115.51	116.34	106.79	88.15	67.81	50.36	37.94	28.76	22.61
	0.10	70.82	78.39	85.99	87.15	84.26	77.77	69.33	60.60	52.25	44.62
		68.04	74.95	78.25	76.86	69.89	59.15	47.23	37.31	29.18	23.27
	0.125	47.89	52.45	56.47	58.42	57.74	54.73	50.79	45.08	41.09	36.34
c_S		45.24	49.09	51.76	52.70	50.80	46.57	40.56	34.07	28.15	23.16
	0.15	33.94	36.63	38.86	39.67	40.11	39.18	37.26	34.20	31.80	28.79

(*Continues*)

Table IV. Continued.

					c_S					
		31.36	33.35	34.87	35.70	35.73	34.59	32.08	28.80	25.26	21.73
	0.175	25.06	26.92	27.40	28.40	28.64	28.12	27.34	26.22	24.60	22.87
		23.19	24.24	25.05	25.57	25.78	25.49	24.57	22.97	21.23	19.17
	0.20	19.16	20.17	20.97	21.50	21.68	21.48	20.69	20.36	19.41	18.25
		17.70	18.25	18.74	19.15	19.35	19.29	18.85	18.20	17.27	16.21
	0.225	15.37	16.04	16.41	16.75	16.94	16.78	16.73	16.09	15.63	14.99
		14.12	14.41	14.68	14.87	14.97	14.93	14.75	14.47	14.05	13.51
	0.25	12.60	13.02	13.28	13.49	13.59	13.47	13.43	13.20	12.82	12.51
		11.65	11.82	11.95	12.02	12.08	12.11	12.04	11.92	11.71	11.41
						c_ε					
		1.10	1.20	1.30	1.40	1.50	1.60	1.80	2.20	2.60	3.00
	−0.025	95.83	48.62	27.94	18.46	13.25	9.99	6.75	4.08	2.95	2.33
		102.10	54.03	31.22	20.40	14.59	11.11	7.46	4.46	3.21	2.54
	−0.05	80.35	44.43	26.81	17.74	12.92	10.06	6.74	4.08	2.96	2.34
		85.78	49.09	29.97	19.78	14.33	11.01	7.42	4.46	3.21	2.54
	−0.075	63.10	38.32	24.76	16.93	12.45	9.74	6.62	4.05	2.95	2.34
		67.07	42.26	27.27	18.76	13.83	10.77	7.34	4.44	3.21	2.54
	−0.10	47.47	31.72	21.70	15.63	11.79	9.29	6.54	4.05	2.94	2.33
		49.77	34.77	24.04	17.41	13.17	10.42	7.20	4.42	3.20	2.54
	−0.125	36.31	26.16	18.88	14.29	11.20	8.99	6.39	4.01	2.92	2.33
c_S		36.87	27.99	20.87	15.79	12.36	9.99	7.05	4.37	3.18	2.53
	−0.15	27.92	21.35	16.44	12.89	10.32	8.66	6.23	3.97	2.91	2.31
		27.57	22.46	18.01	14.26	11.46	9.48	6.85	4.32	3.16	2.53
	−0.175	21.92	17.85	14.34	11.50	9.59	8.08	6.01	3.93	2.90	2.32
		21.19	18.33	15.38	12.80	10.58	8.97	6.65	4.27	3.15	2.51
	−0.20	17.46	14.80	12.40	10.43	8.82	7.58	5.79	3.84	2.86	2.31
		16.78	15.06	13.25	11.38	9.75	8.42	6.39	4.21	3.13	2.51
	−0.225	14.40	12.73	10.90	9.52	8.17	7.10	5.56	3.78	2.87	2.29
		13.62	12.64	11.44	10.18	8.96	7.90	6.15	4.15	3.10	2.49
	−0.25	12.18	10.91	9.68	8.63	7.56	6.67	5.39	3.70	2.80	2.28
		11.38	10.80	10.04	9.14	8.24	7.36	5.89	4.08	3.07	2.48

$$v_k^2(\widetilde{\tau} - \tau) = O_p(1), \tag{9}$$

where v_k^2 is the related magnitude of change in the parameters. The details of the proof are too technical and hence are omitted. Interested readers can refer to Wang[52] or acquire them on request.

In this article, we use simulations to evaluate the effectiveness of the change point estimate (Equation (8)). We set the change point $\tau = 100$ and the repetitions of simulations equal to 50,000. Any repetition where an OC signal occurs before the $(\tau + 1)$th profile was discarded. The average (avg) and standard deviation (SD) of the estimate $\widetilde{\tau}$ for the shift in intercept, slope, and standard deviation of the ZTW chart and the COM charts under Equation (2) for $\sigma_\delta^2 = 0.1$ and 0.25 are tabulated in Table V, which also report the simulated probabilities P0=$Pr\{\widetilde{\tau} = \tau\}$, P1=$Pr\{|\widetilde{\tau} - \tau| \leqslant 1\}$, P3=$Pr\{|\widetilde{\tau} - \tau| \leqslant 3\}$, and P5=$Pr\{|\widetilde{\tau} - \tau| \leqslant 5\}$. These probabilities are used to assess certain degree of the precision of the estimate $\widetilde{\tau}$.

From Table V, we conclude that the estimate $\widetilde{\tau}$ performs fairly well for any shift size and gives similar results for both the ZTW chart and the COM charts. The estimate $\widetilde{\tau}$ has better precision when the shift in parameter is large. Also, it seems that $\widetilde{\tau}$ would overestimate τ when the shift is small, whereas it would slightly underestimate τ when the shift is large. These findings on the estimate $\widetilde{\tau}$ for the simple linear Berkson profile are consistent with those of Zou *et al.*[10] for the simple linear profile. The precision of $\widetilde{\tau}$, as expected, deteriorates when all the settings are the same except that σ_δ^2 increases from 0.1 to 0.25.

After finding the location of the change point, it is also important to decide which parameters have changed in the profile. Kim *et al.*[3] proposed a combination of three EWMA charts for monitoring the simple linear profile and each chart monitors the corresponding parameter. This approach makes the diagnosis of any profile change much easier than other approaches. However, as the chart for monitoring the intercept or the slope has detected an OC signal, users will usually conceive that the corresponding parameter has changed and disregard the possibility that the signal may have been caused by the parameter of standard deviation. As Reynolds and Stoumbos[53] pointed out, the control charts used as a diagnostic aids do not necessarily have to be the same control charts used to decide when a signal triggers. Hawkins and Zamba[41] used two parametric tests to decide if the shift results from the mean or from the variance. Zou *et al.*[10] used a parametric test method as an auxiliary tool to determine which parameters have shifted in a profile after the chart has detected an OC signal. Following the same line, in this article, we also propose an auxiliary parametric test method to determine which parameters have changed in a profile once the chart has detected a signal.

Table V. The average, standard deviation, and precision of change point estimates for the ZTW chart (first row) and the COM charts (second row)

			σ_δ^2=0.1						σ_δ^2=0.25			
			$B_0 \to B_0 + c_I\sigma_\varepsilon$						$B_0 \to B_0 + c_I\sigma_\varepsilon$			
c_I	$\widetilde{\tau}_{avg}$	$SD_{\widetilde{\tau}}$	P0	P1	P3	P5	c_I	$\widetilde{\tau}_{avg}$	$SD_{\widetilde{\tau}}$	P0	P1	P3	P5
0.40	103.44	15.89	0.11	0.23	0.39	0.50	0.4	105.62	20.20	0.08	0.18	0.32	0.42
	102.76	16.40	0.11	0.23	0.40	0.51		104.94	20.74	0.08	0.18	0.32	0.42
0.80	99.38	8.15	0.34	0.56	0.77	0.87	0.8	99.48	9.51	0.27	0.47	0.69	0.80
	99.15	8.89	0.34	0.57	0.77	0.86		99.20	10.14	0.27	0.48	0.69	0.80
1.20	99.32	5.70	0.56	0.79	0.92	0.96	1.2	99.07	6.97	0.47	0.70	0.87	0.93
	99.20	6.22	0.56	0.79	0.92	0.95		98.93	7.58	0.47	0.70	0.87	0.93
1.60	99.54	4.11	0.73	0.90	0.96	0.98	1.6	99.27	5.48	0.63	0.84	0.94	0.96
	99.45	4.73	0.73	0.90	0.96	0.97		99.18	5.73	0.64	0.84	0.94	0.96
2.00	99.71	3.00	0.84	0.95	0.98	0.99	2	99.52	3.93	0.76	0.91	0.97	0.98
	99.66	3.41	0.85	0.95	0.98	0.98		99.45	4.39	0.76	0.91	0.96	0.98
			$B_1 \to B_1 + c_S\sigma_\varepsilon$						$B_1 \to B_1 + c_S\sigma_\varepsilon$			
c_S	$\widetilde{\tau}_{avg}$	$SD_{\widetilde{\tau}}$	P0	P1	P3	P5	c_S	$\widetilde{\tau}_{avg}$	$SD_{\widetilde{\tau}}$	P0	P1	P3	P5
0.10	118.73	36.68	0.04	0.09	0.18	0.24	0.10	125.55	45.44	0.03	0.07	0.15	0.20
	117.88	37.15	0.04	0.09	0.18	0.24		124.86	46.02	0.03	0.08	0.15	0.20
0.15	105.80	19.83	0.08	0.18	0.32	0.42	0.15	108.66	24.82	0.06	0.14	0.27	0.35
	105.48	20.28	0.08	0.18	0.32	0.42		108.19	25.09	0.06	0.15	0.27	0.35
0.20	101.90	13.84	0.14	0.28	0.46	0.58	0.20	103.03	16.84	0.11	0.23	0.39	0.50
	101.53	14.38	0.14	0.28	0.46	0.58		102.82	17.32	0.11	0.23	0.39	0.50
0.25	100.36	11.05	0.20	0.38	0.58	0.70	0.25	100.89	13.24	0.15	0.31	0.50	0.62
	100.11	11.56	0.20	0.38	0.58	0.70		100.56	13.62	0.16	0.31	0.51	0.62
0.30	99.68	9.44	0.26	0.47	0.68	0.80	0.30	99.86	11.19	0.21	0.39	0.60	0.72
	99.37	10.25	0.26	0.47	0.68	0.80		99.63	11.64	0.21	0.40	0.60	0.72
			$\sigma_\varepsilon \to c_\varepsilon\sigma_\varepsilon$						$\sigma_\varepsilon \to c_\varepsilon\sigma_\varepsilon$			
c_ε	$\widetilde{\tau}_{avg}$	$SD_{\widetilde{\tau}}$	P0	P1	P3	P5	c_ε	$\widetilde{\tau}_{avg}$	$SD_{\widetilde{\tau}}$	P0	P1	P3	P5
1.4	102.01	13.90	0.13	0.28	0.47	0.59	1.4	105.91	19.55	0.08	0.18	0.33	0.43
	101.80	14.21	0.14	0.28	0.47	0.59		105.33	19.82	0.08	0.19	0.34	0.44
1.8	99.53	7.94	0.34	0.57	0.79	0.88	1.8	100.00	9.55	0.24	0.45	0.67	0.78
	99.58	7.86	0.35	0.58	0.79	0.88		99.95	9.58	0.25	0.46	0.67	0.79
2.2	99.51	5.84	0.51	0.75	0.91	0.95	2.2	99.46	7.16	0.40	0.64	0.84	0.91
	99.56	5.67	0.52	0.76	0.91	0.95		99.50	7.10	0.41	0.65	0.84	0.91
2.6	99.66	4.41	0.63	0.85	0.95	0.97	2.6	99.51	5.66	0.52	0.76	0.91	0.95
	99.71	3.98	0.64	0.85	0.95	0.97		99.55	5.57	0.53	0.77	0.92	0.96
3	99.75	3.48	0.72	0.90	0.97	0.98	3	99.65	4.44	0.62	0.84	0.95	0.97
	99.75	3.52	0.72	0.91	0.97	0.98		99.68	4.23	0.63	0.85	0.95	0.97

Assume that an OC signal has been detected at kth profile. After obtaining the change point estimate $\widetilde{\tau}$ in Equation (8), define

$$\check{B}_0 = \frac{1}{n(k-\widetilde{\tau})}\sum_{j=\widetilde{\tau}+1}^{k}\sum_{i=1}^{n} y_{ij}, \check{B}_1 = \frac{1}{k-\widetilde{\tau}}\sum_{j=\widetilde{\tau}+1}^{k}\sum_{i=1}^{n}\frac{x_i^* y_{ij}}{S_{xx}},$$

$$\check{\sigma}^2 = \frac{1}{n(k-\widetilde{\tau})-2}\sum_{j=\widetilde{\tau}+1}^{k}\sum_{i=1}^{n}\left(y_{ij}-\check{B}_0-\check{B}_1 x_i^*\right)^2,$$

and

$$\check{\sigma}_\varepsilon^2 = \max\left\{0, \check{\sigma}^2 - \check{B}_1^2\sigma_\delta^2\right\}.$$

For an intercept change and a slope change, we used the t-test with $n(k-\widetilde{\tau})-2$ degrees of freedom, and the respective test statistics are

$$T_I = \frac{\sqrt{n(k-\widetilde{\tau})}\left(\check{B}_0 - B_0\right)}{\check{\sigma}} \tag{10}$$

and

$$T_S = \frac{\sqrt{S_{xx}(k-\tilde{\tau})}\left(\check{B}_1 - B_1\right)}{\check{\sigma}} \tag{11}$$

For a change in σ_ε^2, we use the test statistic

$$T_{\sigma_\varepsilon} = \frac{\check{\sigma}_\varepsilon^2 - \sigma_\varepsilon^2}{\sqrt{\widehat{\mathrm{Var}}\left(\check{\sigma}_\varepsilon^2\right)}}, \tag{12}$$

where

$$\widehat{\mathrm{Var}}\left(\check{\sigma}_\varepsilon^2\right) = \frac{2\left(\sigma_\varepsilon^2 + \check{B}_1^2\sigma_\delta^2\right)^2}{n(k-\tilde{\tau})} + \frac{4\check{B}_1^2\sigma_\delta^4\left(\sigma_\varepsilon^2 + \check{B}_1^2\sigma_\delta^2\right)}{S_{xx}(k-\tilde{\tau})}.$$

Here, we substitute $\check{B}_1$ for B_1 in $\widehat{\mathrm{Var}}\left(\check{\sigma}_\varepsilon^2\right)$ so that a change in B_1 will not affect the result for testing a change in σ_ε^2. It is easy to show that T_{σ_ε} has an asymptotic standard normal distribution under the condition that $S_{xx}/n \to S_{xx}^* < \infty$, and there is no change in σ_ε^2.

In this article, we present the diagnostic ability of identifying OC parameters using the aforementioned hypothesis test method with $\alpha = 0.05$ for the ZTW chart and the COM charts. The results are obtained using 50,000 simulations and are tabulated in Table VI. The three digits in the second row of the table indicate various combinations of parameter shifts in the intercept B_0, slope B_1, and standard deviation σ_ε. For example, the three digits '100' represent the intercept, slope, and standard deviation, where the first digit '1' means a shift in the intercept B_0 and the other two digits '00' mean no change in the slope B_1 and standard deviation σ_ε. The estimated probabilities of events occurring at '100', '010', and so on for various shifts are reported. The larger probabilities imply the better diagnostic ability of the parametric tests for the control charts.

Table VI shows that for a single shift in the parameter, except for few cases when $c_I = c_S = 0$, the proposed hypothesis test method is more accurate for the COM charts than for the ZTW chart. For simultaneous shifts in the intercept and slope, the proposed hypothesis test method is not very effective for both the ZTW chart and the COM charts because if there is a larger degree of shift in one of the two parameters, the test method tends to indicate that there is only one parameter has changed. This phenomenon is even more serious for simultaneous shifts in three parameters. Overall, the proposed hypothesis test method is more effective for the COM charts than for the ZTW chart in terms of diagnostic ability.

It should be noted that the proposed hypothesis test statistics do not exactly have the given null distributions as the process is in control because the statistics are derived on the basis of the condition that the control charts have detected an OC signal and a change point estimate have been obtained. In addition, the efficiency of the hypothesis test method depends on when the control chart has detected an OC signal and the accuracy of the estimate of the change point. Therefore, although this diagnostic method is useful in many situations, users still have to take engineering/practical knowledge about the profile into account after they have obtained the results from statistical diagnostic analysis.

5. An illustrative example

In this section, we use an example of Montgomery[54] (p. 477) to illustrate the applicability and the implementation of the proposed methodology. In a semiconductor manufacturing process, during the etch step, a wafer is put in a chamber and exposed to gases that etch away photoresist, thus creating the required pattern for that layer of the chips. The quality of the process is characterized by the relationship between the measured pressure (psi) and the flow of gases (cm^3) in the chamber, controlled by a mass flow controller (MFC). According to physical principles, if an MFC is in control, then the measured pressure y is approximately a linear function of the flow of gases ξ in the chamber. However, because of random fluctuations in gases, it is likely that the set point value for flow x (expressed as a fraction of maximum flow) is different from the actual value of flow ξ in the chamber. If the difference between the set point value for flow x and the actual value of flow ξ in the chamber is too large to be disregarded, that is, x is equal to ξ plus a random error δ, then the simple linear Berkson Equation (1) should be used instead of the simple linear model. The original data that contain the measured pressure y in psi and the set point x for flow in cubic centimeters are presented in Figure 1. In the example, because the book does not include the values of data set, we respectively partition both the pressure and the flow coordinates of Figure 1 into a grid of distinguishable values to collect the approximate integer values of the pressure and flow presented in Table VII. Here, we assume that the values of flow are the set point values for flow controlled by the experimenter, which are appreciably different from the actual values of flow in the chamber, and as a result we can assume a simple linear Berkson model to illustrate our proposed approach. Fitting the simple linear Equation (2) for the values of pressure and flow (coded so that the average value is 0), we have $B_0 = 56.2$, $B_1 = 0.22$, and $\sigma^2 = \sigma_\varepsilon^2 + B_1^2\sigma_\delta^2 = 3.94$. Further, we assume $\sigma_\delta^2 = 0.25\sigma_\varepsilon^2 = 0.97$, which indicates that there is an appreciable difference between the set point value for flow and the actual value of flow in the chamber. As a result, we have the following in-control simple linear Berkson model

$$\begin{aligned} y &= 56.2 + 0.22\xi + \varepsilon, \\ x &= \xi + \delta, \end{aligned} \tag{13}$$

where $\varepsilon \sim N(0, 3.89)$, $\delta \sim N(0, 0.97)$, and ε and δ are independent. To start a Phase II monitoring, we choose the IC ARL = 200 and the

Table VI. Diagnostic abilities of the parametric test method for shifts in B_0, B_1, and σ_ε^2 using the ZTW chart (first row) and the COM charts (second row)

					σ_δ^2=0.1					
c_I	c_S	c_ε	100	010	001	110	101	011	111	000
0.4	0	1	0.68	0.03	0.03	0.16	0.07	0.00	0.01	0.01
			0.74	0.02	0.02	0.13	0.07	0.00	0.01	0.02
0.8	0	1	0.77	0.01	0.02	0.13	0.05	0.00	0.01	0.01
			0.79	0.00	0.01	0.11	0.06	0.00	0.01	0.01
0	0.1	1	0.07	0.58	0.05	0.18	0.01	0.07	0.02	0.02
			0.07	0.65	0.04	0.13	0.01	0.07	0.01	0.02
0	0.15	1	0.04	0.64	0.04	0.17	0.00	0.07	0.01	0.02
			0.03	0.72	0.03	0.12	0.00	0.07	0.01	0.02
0	0	0.4	0.00	0.00	0.82	0.00	0.08	0.08	0.01	0.00
			0.00	0.00	0.80	0.00	0.09	0.09	0.01	0.00
0	0	0.7	0.01	0.01	0.77	0.01	0.09	0.08	0.02	0.00
			0.01	0.01	0.75	0.01	0.10	0.10	0.02	0.01
0	0	1.6	0.06	0.06	0.70	0.03	0.06	0.06	0.00	0.02
			0.06	0.06	0.70	0.02	0.07	0.07	0.00	0.01
0	0	2.8	0.03	0.03	0.82	0.02	0.04	0.04	0.00	0.03
			0.03	0.03	0.81	0.02	0.04	0.04	0.00	0.02
0.6	0.15	1	0.44	0.07	0.03	0.38	0.04	0.01	0.02	0.02
			0.47	0.06	0.01	0.38	0.04	0.00	0.02	0.01
0.6	0.15	1.6	0.17	0.08	0.41	0.09	0.15	0.04	0.01	0.04
			0.17	0.08	0.35	0.09	0.21	0.06	0.02	0.03
0.4	0.15	2	0.06	0.07	0.67	0.04	0.08	0.05	0.00	0.04
			0.06	0.07	0.64	0.03	0.10	0.07	0.01	0.02
					σ_δ^2=0.25					
c_I	c_S	c_ε	100	010	001	110	101	011	111	000
0.4	0	1	0.67	0.03	0.03	0.17	0.07	0.01	0.01	0.01
			0.73	0.03	0.02	0.12	0.07	0.00	0.01	0.01
0.8	0	1	0.76	0.01	0.02	0.13	0.05	0.00	0.00	0.01
			0.79	0.01	0.01	0.11	0.05	0.00	0.01	0.01
0	0.1	1	0.09	0.55	0.07	0.18	0.01	0.06	0.01	0.03
			0.10	0.62	0.06	0.12	0.01	0.06	0.01	0.02
0	0.15	1	0.06	0.63	0.05	0.16	0.01	0.05	0.01	0.03
			0.05	0.70	0.04	0.12	0.00	0.05	0.01	0.02
0	0	0.4	0.01	0.01	0.80	0.01	0.08	0.07	0.01	0.01
			0.01	0.01	0.77	0.01	0.09	0.08	0.01	0.01
0	0	0.7	0.03	0.03	0.70	0.04	0.09	0.08	0.02	0.01
			0.03	0.03	0.71	0.01	0.09	0.09	0.01	0.02
0	0	1.6	0.07	0.07	0.65	0.04	0.06	0.07	0.00	0.03
			0.07	0.07	0.66	0.03	0.07	0.07	0.01	0.02
0	0	2.8	0.04	0.04	0.79	0.02	0.04	0.04	0.00	0.03
			0.03	0.04	0.79	0.02	0.05	0.05	0.00	0.02
0.6	0.15	1	0.46	0.09	0.03	0.35	0.03	0.00	0.01	0.03
			0.48	0.08	0.02	0.34	0.04	0.00	0.02	0.02
0.6	0.15	1.6	0.22	0.11	0.34	0.10	0.14	0.03	0.00	0.05
			0.22	0.11	0.28	0.11	0.20	0.04	0.02	0.03
0.4	0.15	2	0.08	0.09	0.61	0.04	0.08	0.04	0.01	0.05
			0.08	0.09	0.59	0.04	0.10	0.06	0.01	0.03

smoothing constant $\lambda = 0.2$ for the proposed COM control charts. For the first five in-control profiles, we generate profile data from Equation (13) with sample size $n = 20$ and x_i equal to the set point values for flow in Table VII. After the fifth profile, we add a shift of B_1 on the in-control model from 0.22 to 0.23 and generate the OC profiles through Monte Carlo simulations. The simulated y_{ij} for $i = 1, \cdots, 20$ and $j = 1, \cdots, 12$ are tabulated in Table VIII.

Figure 2 gives the COM charts for monitoring these in-control and OC sample profiles, which include $EWMA_I$ for the change in B_0, $EWMA_S$ for the change in B_1, $EWMA_c^+$ for the increase in σ_ε, and $EWMA_c^-$ for the decrease in σ_ε. Note that the magnitude of shift in these profiles is usually small and difficult to identify by bare eyes. Thus, we need an effective control charting scheme to discover the slight change. From Figure 2, we observe that the COM charts trigger a signal quickly at the 12th profile. Using the diagnostic

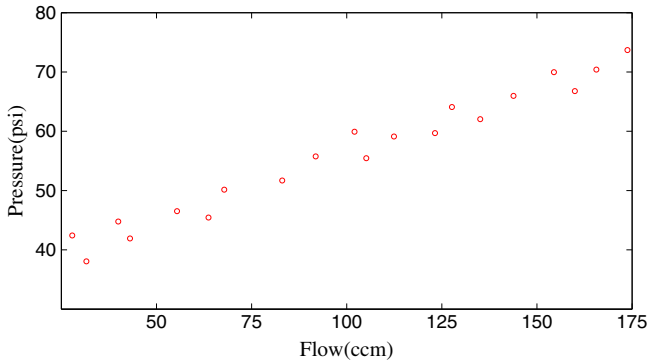

Figure 1. The measured pressure for an MFC is expressed as a function of the set point x for flow.

Table VII. Approximate values of the data set for the MFC example of Montgomery (2009)

Pressure y (psi)	42	38	45	42	47	45	50	52	56	60
Flow x (cm^3)	28	32	40	43	55	64	68	83	92	102
Pressure y (psi)	55	59	60	64	62	66	70	67	70	74
Flow x (cm^3)	105	112	123	128	135	144	154	160	166	174

Table VIII. Data for illustrative example with a shift in B_1 after the fifth profile

j	0	1	2	3	4	5	6	7	8	9	10	11	12
		37.13	42.95	43.56	39.66	35.33	37.42	40.19	39.08	37.32	42.18	35.90	39.47
		39.64	41.04	40.11	43.21	42.76	40.23	38.77	43.33	37.61	40.07	41.57	39.58
		43.55	42.49	43.21	42.38	43.20	40.63	40.61	44.80	42.14	42.79	42.20	41.82
		43.63	45.27	44.77	40.79	43.02	44.08	42.90	40.43	44.44	44.91	42.05	43.78
		47.00	47.43	41.88	44.36	50.71	45.65	45.50	48.64	45.83	44.86	46.20	47.67
		49.46	47.00	46.37	46.18	49.64	47.72	45.25	45.50	48.65	48.58	47.98	48.18
		48.10	46.84	48.67	49.41	49.15	46.83	45.69	47.70	48.05	49.48	48.62	44.40
		50.50	52.56	52.23	54.12	50.58	52.86	52.30	50.65	52.76	51.79	53.61	55.04
y_{ij}		54.68	54.70	55.04	52.06	52.84	55.03	51.48	56.40	57.69	53.46	55.35	55.87
		56.19	54.94	54.11	56.85	57.21	57.09	56.94	54.46	56.47	59.23	54.64	54.82
		55.89	58.21	60.39	59.43	55.23	55.57	60.11	56.85	57.48	60.67	57.99	59.84
		57.59	53.44	58.44	57.93	59.98	58.37	57.79	61.33	60.92	59.40	56.76	62.25
		58.90	59.24	61.65	60.54	63.79	60.01	59.10	66.11	63.29	59.41	60.34	59.51
		63.06	66.24	61.94	58.71	62.91	63.45	61.54	62.66	61.31	62.88	60.88	63.19
		62.59	61.15	63.62	66.90	61.65	63.66	65.90	64.87	63.83	64.33	64.12	69.59
		65.84	65.97	68.27	72.14	62.23	63.31	66.40	67.15	65.81	69.31	67.97	64.56
		71.44	69.02	67.94	65.54	67.13	71.79	66.63	68.45	67.84	68.48	68.47	68.03
		70.14	69.08	69.47	69.86	67.52	71.25	68.11	68.41	69.90	70.32	66.91	71.39
		71.14	68.21	73.37	71.51	70.17	72.29	70.08	69.61	74.46	73.59	70.42	71.14
		73.52	76.02	70.38	71.90	71.88	75.59	71.38	71.17	73.31	69.30	74.39	75.21
lr	10.81	8.58	10.47	10.59	10.20	14.87	8.97	9.03	10.58	5.30	4.96	5.61	

method, we proposed for the simple linear Berkson model; we have the values of $lr(20j, 12 \times 20), j = 0, 1, \cdots, 11$, tabulated in Table VIII. From the table, we see that $lr(20j, 12 \times 20)$ attains its maximum value at $j = 5$ with $lr(20 \times 5, 12 \times 20) = 14.87$. Thus, the change point estimate $\tilde{\tau} = 5$ in this case, which is identical to the actual change point.

After obtaining the change point estimate $\tilde{\tau}$, we compute the test statistics in Equations (10), (11), and (12) to obtain $T_I = 0.23$, $T_S = 3.83$, and $T_{\sigma_\varepsilon} = -1.43$. Considering the significance level $\alpha = 0.05$, we see that $|T_I| = 0.23 < t_{0.025}(138) = 1.98$, $|T_S| = 3.83 > t_{0.025}(138) = 1.98$, and $|T_{\sigma_\varepsilon}| = 1.43 < z_{0.025} = 1.96$, where $t_\alpha(v)$ and z_α are the respective α upper quantiles of the t distribution with v degrees of freedom and of the standard normal distribution. From this, we conclude that there is a slope shift after the fifth profile. After discovering the OC parameter, the user may try to find the assignable causes and repair the process. When the process is adjusted back to normal condition, the monitoring procedure can be restarted again.

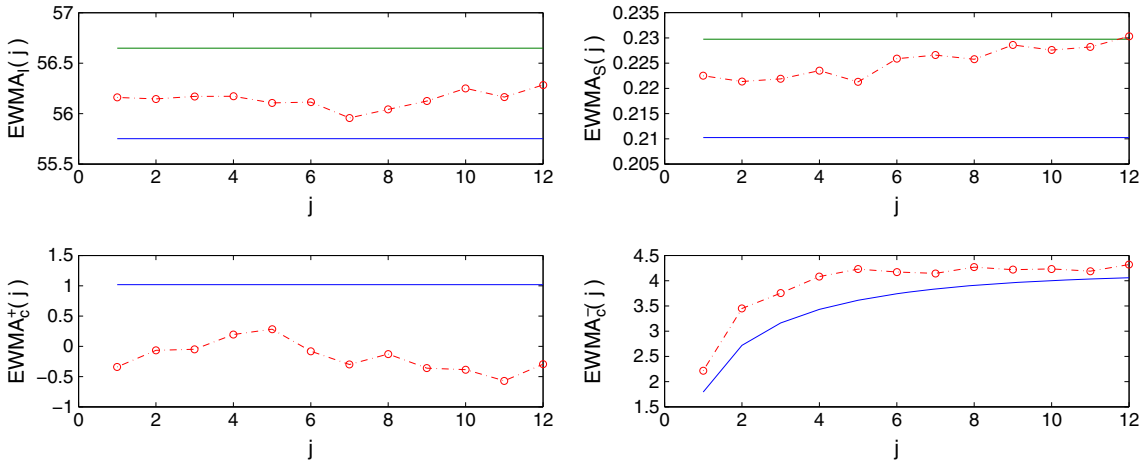

Figure 2. The COM charts for monitoring the intercept, slope, and standard deviation.

6. Conclusion

In this article, by making use of the transformed simple linear profile, we have studied three control charting schemes for monitoring a simple linear Berkson profile. These charting schemes can be generalized to monitor a multiple linear Berkson profile, which has several explanatory variables and different identifiability conditions. According to the performance comparisons, the ZTW chart and the COM charts are the two preferred schemes among the three in terms of the OC ARL. We have also given a systematic diagnostic method to estimate the change point and to identify which parameters have changed in the profile. On the basis of the simulation results of comparing the diagnostic ability of indicating OC parameters between the ZTW chart and the COM charts, the COM charts give slightly better results. As illustrated by the MFC example, the COM control charts and its corresponding diagnostic approach can be implemented in industrial practice under the situation that the quality of a process can be represented by a simple linear Berkson profile.

Acknowledgements

The authors thank the editor and two anonymous referees for their many helpful comments that have resulted in significant improvements in the article. The authors also thank the support of NCTS of National Tsing Hua University in Taiwan.

References

1. Woodall WH, Spitzner DJ, Montgomery DC, Gupta S. Using control charts to monitor process and product quality profiles. *Journal of Quality Technology* 2004; **36**:309–320.
2. Kang L, Albin SL. On-line monitoring when the process yields a linear profile. *Journal of Quality Technology* 2000; **32**:418–426.
3. Kim K, Mahmoud MA, Woodall WH. On the monitoring of linear profiles. *Journal of Quality Technology* 2003; **35**:317–328.
4. Gupta S, Montgomery DC, Woodall WH. Performance evaluation of two methods for online monitoring of linear calibration profiles. *International Journal of Production Research* 2006; **44**:1927–1942.
5. Croarkin C, Varner R. Measurement assurance for dimensional measurements on integrated-circuit photomasks. NBS Technical Note 1164, U.S. Department of Commerce, 1982.
6. Mahmoud MA, Woodall WH. Phase I monitoring of linear profiles with calibration application. *Technometrics* 2004; **46**:380–391.
7. Zou C, Zhang Y, Wang Z. Control chart based on change-point model for monitoring linear profiles. *IIE Transactions* 2006; **38**:1093–1103.
8. Mahmoud MA, Parker PA, Woodall WH, Hawkins DM. A change point method for linear profile data. *Quality and Reliability Engineering International* 2007; **23**:247–268.
9. Zou C, Zhou C, Wang X, Tsung F. A self-starting control chart for linear profiles. *Journal of Quality Technology* 2007; **39**:364–375.
10. Zou C, Tsung F, Wang Z. Monitoring general linear profiles using multivariate exponentially weighted moving average schemes. *Technometrics* 2007; **49**:395–408.
11. Jesen DR, Hui YV, Ghare PM. Monitoring an input-output model for production. I: The control charts. *Management Science* 1984; **30**:1197–1206.
12. Mestek O, Pavlik J, Suchanek M. Multivariate control charts: Control charts for calibration curves. *Journal of Analytical Chemistry* 1994; **350**:344–351.
13. Stover FS, Brill RV. Statistical quality control applied to ionchromatography calibrations. *Journal of Chromatography. A* 1998; **804**:37–43.
14. Lawless JF, Mackay RJ, Robinson JA. Analysis of variation transmission in manufacturing process, part I. *Journal of Quality Technology* 1999; **31**:131–142.
15. Walker E, Wright S. Comparing curves using additive models. *Journal of Quality Technology* 2002; **34**:118–129.
16. Williams JD, Woodall WH, Birch JB. Statistical monitoring of nonlinear product and process quality profiles. *Quality and Reliability Engineering International* 2007; **23**:925–941.

17. Colosimo BM, Pacella M. On the use of principal component analysis to identify systematic patterns in roundness profiles. *Quality and Reliability Engineering International* 2007; **23**:707–725.
18. Williams JD, Birch JB, Woodall WH, Ferry NM. Statistical monitoring of heteroscedastic dose–response profiles from high-throughput screening. *Journal of Agricultural, Biological, and Environmental Statistics* 2007; **12**:216–235.
19. Jin J, Shi J. Feature-preserving data compression of stamping tonnage information using wavelet. *Technometrics* 1999; **41**:327–339.
20. Lada EK, Lu J-C, Wilson JR. A wavelet-based procedure for process fault detection. *IEEE Transactions on Semiconductor Manufacturing* 2002; **15**:79–90.
21. Ding Y, Zeng L, Zhou S. Phase I analysis for monitoring nonlinear profiles in manufacturing processes. *Journal of Quality Technology* 2006; **38**:199–216.
22. Zou C, Tsung F, Wang Z. Monitoring profiles based on nonparametric regression methods. *Technometrics* 2008; **50**:512–526.
23. Fan J, Zhang C, Zhang J. Generalized likelihood ratio statistics and Wilks phenomenon. *The Annals of Statistics* 2001; **29**:153–193.
24. Fan J, Gijbels I. Local Polynomial Modeling and Its Applications. Chapman & Hall: London, 1996.
25. Qiu P, Zou C, Wang Z. Nonparametric profile monitoring by mixed effects modeling. *Technometrics* 2010; **52**:265–293.
26. Berkson J. Are there two regressions? *Journal of the American Statistical Association* 1950; **45**:164–180.
27. Rosner B, Willett WC, Spiegelman D. Correction of logistic regression relative risk estimates and confidence intervals for systematic within-person measurement error. *Statistics in Medicine* 1989; **8**:1051–1069.
28. Rosner B, Spiegelman D, Willett WC. Correction of logistic regression relative risk estimates and confidence intervals for measurement error: The case of multiple covariates measured with error. *American Journal of Epidemiology* 1990; **132**:734–745.
29. Tosteson TD, Stefanski LA, Schafer DW. A measurement error model for binary and ordinal regression. *Statistics in Medicine* 1989; **8**:1139–1147.
30. Schafer DW, Gilbert ES. Some statistical implications of dose uncertainty in radiation dose–response analyses. *Radiation Research* 2006; **166**:303–312.
31. Quesenberry CP. On properties of Q charts for variables. *Journal of Quality Technology* 1995; **27**:184–203.
32. Chen G, Cheng SW, Xie H. Monitoring process mean and variability with one EWMA chart. *Journal of Quality Technology* 2001; **33**:223–233.
33. Lowry CA, Woodall WH, Champ CW, Rigdon SE. A multivariate exponentially weighted moving average control chart. *Technometrics* 1992; **34**:46–53.
34. Huwang L, Wang YT, Yeh AB, Chen, ZJ. On the exponentially weighted moving variance. *Naval Research Logistics* 2009; **56**:659–668.
35. Box GEP. Some theorems on quadratic forms applied in the study of analysis of variance problems: Effect on inequality of variance in one-way classification. *Annals of Mathematical Statistics* 1954; **25**:290–302.
36. Lawless JF. Statistical Models and Methods for Lifetime Data (2nd edn). Wiley: New York, 2003.
37. Shu L, Jiang WA. new EWMA chart for monitoring process dispersion. *Journal of Quality Technology* 2008; **40**:319–331.
38. Acosta-Mejia CA. Monitoring process dispersion. *Ph.D. Dissertation*, Texas A&M University, College Station, Texas, 1995.
39. Acosta-Mejia CA, Pignatiello JJ Jr. Monitoring Process Dispersion without Subgrouping. *Journal of Quality Technology* 2000; **32**:89–102.
40. Hawkins DM, Qiu P, Kang CW. The changepoint model for statistical process control. *Journal of Quality Technology* 2003; **35**:355–366.
41. Hawkins DM, Zamba KD. Statistical process control for shifts in mean or variance using a change-point formulation. *Technometrics* 2005; **47**:164–173.
42. Hawkins DM, Zamba KD. A change-point model for a shift in variance. *Journal of Quality Technology* 2005; **37**:21–31.
43. Pignatiello JJ JR, Samuel TR. Estimation of the change point of a normal process mean in SPC applications. *Journal of Quality Technology* 2001; **33**:82–95.
44. Andrews DWK. Testing for parameter instability and structural change with unknown change point. *Econometrica* 1993; **61**:821–856.
45. Bai J. Estimation of a change point in multiple regression models. *The Review of Economics and Statistics* 1997; **79**:551–563.
46. Csörgő M, Horváth L. Limit theorems in change-point analysis. Wiley Series in Probability and Statistics, Wiley: New York, 1997.
47. Liu J, Wu S, Zidek JV. On segmented multivariate regressions. *Statistica Sinica* 1997; **7**:497–525.
48. Bai J. Likelihood ratio tests for multiple structural changes. *Journal of Econometrics* 1999; **91**:299–323.
49. Bai J, Perron P. Estimating and testing linear models with multiple structural changes. *Econometrica* 1998; **66**:47–78.
50. Bai J, Perron P. Critical values for multiple structural change tests. *The Econometrics Journal* 2003; **6**:72–78.
51. Qu Z, Perron P. Estimating and testing structural changes in multivariate regressions. *Econometrica* 2007; **75**:459–502.
52. Wang YT. On the monitoring of linear Berkson profiles. *Ph.D. Dissertation*, National Tsing Hua University, Hsinchu, Taiwan, 2010.
53. Reynolds MR JR, Stoumbos ZG. Should exponentially weighted moving average and cumulative sum charts be used with Shewhart limits? *Technometrics* 2005; **47**:409–424.
54. Montgomery DC. Introduction to Statistical Quality Control (6th edn). Wiley: New York, 2009.

Appendix

Proof of (8)

Suppose that the control chart has detected an OC signal at the kth profile, the logarithm of the likelihood function for the k profiles is defined by

$$l = -\frac{1}{2}\sum_{j=1}^{k}\left\{n\ln\left[2\pi\left(\sigma_{\varepsilon_j}^2 + B_{1j}^2\sigma_\delta^2\right)\right] + \sum_{i=1}^{n}\frac{\left(y_{ij} - B_{0j} - B_{1j}x_i^*\right)^2}{\sigma_{\varepsilon_j}^2 + B_{1j}^2\sigma_\delta^2}\right\}.$$

If all the k profiles are collected under in-control conditions, the logarithm of the likelihood function is equal to

$$l_0 = -\frac{1}{2}\left\{kn\ln\left[2\pi\left(\sigma_\varepsilon^2 + B_1^2\sigma_\delta^2\right)\right] + \sum_{j=1}^{k}\sum_{i=1}^{n}\frac{\left(y_{ij} - B_0 - B_1x_i^*\right)^2}{\sigma_\varepsilon^2 + B_1^2\sigma_\delta^2}\right\}.$$

Under the condition that a sustained change occurs after the tth profile, the corresponding logarithm of likelihood is given by

$$l_1 = -\frac{1}{2}\left\{ tn\ln\left[2\pi\left(\sigma_\varepsilon^2 + B_1^2\sigma_\delta^2\right)\right] + \sum_{j=1}^{t}\sum_{i=1}^{n}\frac{\left(y_{ij} - B_0 - B_1 x_i^*\right)^2}{\sigma_\varepsilon^2 + B_1^2\sigma_\delta^2}\right\}$$
$$-\frac{1}{2}\left\{ (k-t)n\ln\left[2\pi\left(\sigma_{\varepsilon c}^2 + B_{1c}^2\sigma_\delta^2\right)\right] + \sum_{j=t+1}^{k}\sum_{i=1}^{n}\frac{\left(y_{ij} - B_{0c} - B_{1c}x_i^*\right)^2}{\sigma_{\varepsilon c}^2 + B_{1c}^2\sigma_\delta^2}\right\},$$

where B_{0c}, B_{1c}, and $\sigma_{\varepsilon c}^2$, respectively, represent the corresponding parameters after the change. Taking the partial derivatives of l_1 with respect to B_{0c}, B_{1c}, and $\sigma_{\varepsilon c}^2$, respectively, and solving the equations $\frac{\partial l_1}{\partial B_{0c}} = \frac{\partial l_1}{\partial B_{1c}} = \frac{\partial l_1}{\partial \sigma_{\varepsilon c}^2} = 0$, we have

$$\hat{B}_{0(t,k)} = \frac{1}{n(k-t)}\sum_{j=t+1}^{k}\sum_{i=1}^{n} y_{ij} \equiv \bar{\bar{y}},$$

$$\hat{B}_{1(t,k)} = \frac{1}{(k-t)}\sum_{j=t+1}^{k}\sum_{i=1}^{n}\frac{x_i^* y_{ij}}{S_{xx}},$$

and

$$\hat{\sigma}_{\varepsilon(t,k)}^2 = \frac{\sum_{j=t+1}^{k}\sum_{i=1}^{n}\left(y_{ij} - \hat{B}_{0(t,k)} - \hat{B}_{1(t,k)}x_i^*\right)^2}{n(k-t)} - \hat{B}_{1(t,k)}^2\sigma_\delta^2.$$

Under the condition $\hat{\sigma}_{\varepsilon(t,k)}^2 \geqslant 0$, then $\hat{B}_{0(t,k)}$, $\hat{B}_{1(t,k)}$, and $\hat{\sigma}_{\varepsilon(t,k)}^2$ are the maximum likelihood estimates of B_{0c}, B_{1c} and $\sigma_{\varepsilon c}^2$ respectively. On the other hand, if $\hat{\sigma}_{\varepsilon(t,k)}^2 < 0$, then $\hat{\sigma}_{\varepsilon(t,k)}^2$ is not the maximum likelihood estimate of $\sigma_{\varepsilon c}^2$ because of the restriction $\sigma_{\varepsilon c}^2 \geqslant 0$. From the partial derivative of l_1 with respect to $\sigma_{\varepsilon c}^2$, we have

$$\frac{\partial l_1}{\partial \sigma_{\varepsilon c}^2} = \frac{\sum_{j=t+1}^{k}\sum_{i=1}^{n}\left(y_{ij} - B_{0c} - B_{1c}x_i^*\right)^2/[n(k-t)] - \left(\sigma_{\varepsilon c}^2 + B_{1c}^2\sigma_\delta^2\right)}{2\left(\sigma_{\varepsilon c}^2 + B_{1c}^2\sigma_\delta^2\right)^2/[n(k-t)]}.$$

If the condition $\sum_{j=t+1}^{k}\sum_{i=1}^{n}\left(y_{ij} - B_{0c} - B_{1c}x_i^*\right)^2/[n(k-t)] - B_{1c}^2\sigma_\delta^2 < 0$ holds, then $\frac{\partial l_1}{\partial \sigma_{\varepsilon c}^2} < 0$. As a result, the logarithm of likelihood l_1 is a decreasing function in $\sigma_{\varepsilon c}^2$ and the maximum of l_1 on the region $\sigma_{\varepsilon c}^2 \geqslant 0$ will occur at $\sigma_{\varepsilon c}^2 = 0$. Furthermore, taking the partial derivative of l_1 with respect to B_{0c} and solving $\frac{\partial l_1}{\partial B_{0c}} = 0$, we obtain $\tilde{B}_0 = \hat{B}_{0(t,k)} = \bar{\bar{y}}$. Finally, taking the partial derivative of l_1 with respect to B_{1c} and substituting $B_{0c} = \bar{\bar{y}}$ and $\sigma_{\varepsilon c}^2 = 0$ in $\frac{\partial l_1}{\partial B_{1c}} = 0$, we have

$$-\frac{n(k-t)}{B_{1c}} + \frac{\sum_{j=t+1}^{k}\sum_{i=1}^{n}\left(y_{ij} - \bar{\bar{y}} - B_{1c}x_i^*\right)x_i^*}{B_{1c}^2\sigma_\delta^2} + \frac{\sum_{j=t+1}^{k}\sum_{i=1}^{n}\left(y_{ij} - \bar{\bar{y}} - B_{1c}x_i^*\right)^2}{B_{1c}^3\sigma_\delta^2} = 0.$$

After some simplification, the above equation is equivalent to

$$B_{1c}^2\sigma_\delta^2 + B_{1c}\tilde{S}_{xy} - \tilde{S}_{yy} = 0, \tag{A1}$$

where

$$\tilde{S}_{xy} = \frac{\sum_{j=t+1}^{k}\sum_{i=1}^{n}x_i^*\left(y_{ij} - \bar{\bar{y}}\right)}{n(k-t)}, \tilde{S}_{yy} = \frac{\sum_{j=t+1}^{k}\sum_{i=1}^{n}\left(y_{ij} - \bar{\bar{y}}\right)^2}{n(k-t)}.$$

As a result, under this condition the maximum likelihood estimate of B_{1c} is one of the two solutions of (A1)

$$\tilde{B}_1^{\pm} = \frac{-\tilde{S}_{xy} \pm \sqrt{\tilde{S}_{xy}^2 + 4\sigma_\delta^2\tilde{S}_{yy}}}{2\sigma_\delta^2}.$$

Combining the results for $\hat{\sigma}_{\varepsilon(t,k)}^2 \geqslant 0$ and $\hat{\sigma}_{\varepsilon(t,k)}^2 < 0$, the maximum likelihood estimates of B_{0c}, B_{1c}, and $\sigma_{\varepsilon c}^2$ under the condition that a sustained change occurs after the tth profile are given by

$$\tilde{B}_0 = \bar{\bar{y}},$$

$$\tilde{B}_1 = \begin{cases} \hat{B}_{1(t,k)}, & \hat{\sigma}^2{}_{\varepsilon(t,k)} \geqslant 0, \\ \tilde{B}_1^+, & \hat{\sigma}_{\varepsilon(t,k)}^2 < 0 \text{ and } l_1\left(\tilde{B}_0, \tilde{B}_1^+, 0\right) \geqslant l_1\left(\tilde{B}_0, \tilde{B}_1^-, 0\right), \\ \tilde{B}_1^-, & \hat{\sigma}_{\varepsilon(t,k)}^2 < 0 \text{ and } l_1\left(\tilde{B}_0, \tilde{B}_1^+, 0\right) < l_1\left(\tilde{B}_0, \tilde{B}_1^-, 0\right), \end{cases} \tag{A2}$$

$$\tilde{\sigma}_{\varepsilon}^2 = \max\left[0, \hat{\sigma}_{\varepsilon(t,k)}^2\right].$$

Substituting $\widetilde{B}_0$, $\widetilde{B}_1$, and $\widetilde{\sigma}_{\varepsilon}^2$, respectively, for B_{0c}, B_{1c}, and $\sigma_{\varepsilon c}^2$ in l_1, we have

$$l_1 = -\frac{1}{2}\left\{tn\ln\left[2\pi\left(\sigma_{\varepsilon}^2 + B_1^2\sigma_{\delta}^2\right)\right] + \sum_{j=1}^{t}\sum_{i=1}^{n}\frac{\left(y_{ij} - B_0 - B_1x_i^*\right)^2}{\sigma_{\varepsilon}^2 + B_1^2\sigma_{\delta}^2}\right\}$$
$$-\frac{1}{2}\left\{(k-t)n\ln\left[2\pi\left(\widetilde{\sigma}_{\varepsilon}^2 + \widetilde{B}_1^2\sigma_{\delta}^2\right)\right] + \sum_{j=t+1}^{k}\sum_{i=1}^{n}\frac{\left(y_{ij} - \widetilde{B}_0 - \widetilde{B}_1x_i^*\right)^2}{\widetilde{\sigma}_{\varepsilon}^2 + \widetilde{B}_1^2\sigma_{\delta}^2}\right\}.$$

Consequently, the generalized likelihood ratio statistic is given by

$$lr(tn, kn) = -2(l_0 - l_1)$$
$$= ln\left(\frac{\sigma_{\varepsilon}^2 + B_1^2\sigma_{\delta}^2}{\widetilde{\sigma}_{\varepsilon}^2 + \widetilde{B}_1^2\sigma_{\delta}^2}\right)^{(k-t)n}\left\{\sum_{j=t+1}^{k}\sum_{i=1}^{n}\frac{\left(y_{ij} - B_0 - B_1x_i^*\right)^2}{\sigma_{\varepsilon}^2 + B_1^2\sigma_{\delta}^2} - \sum_{j=t+1}^{k}\sum_{i=1}^{n}\frac{\left(y_{ij} - \widetilde{B}_0 - \widetilde{B}_1x_i^*\right)^2}{\widetilde{\sigma}_{\varepsilon}^2 + \widetilde{B}_1^2\sigma_{\delta}^2}\right\}.$$

Authors' biographies

Dr. Wang is currently an assistant professor in the Department of Statistics of Tamkang University, Taiwan. Her research interest includes data mining and industrial statistics. Her email address is 141110@mail.tku.edu.tw.

Dr. Huwang is currently a professor in the Institute of Statistics of National Tsing Hua University, Taiwan. His research interest includes statistical inference and industrial statistics. His email address is huwang@stat.nthu.edu.tw.